Polymer Bulletin 60, 331–342 (2008)
DOI 10.1007/s00289-007-0871-9

Polymer Bulletin

Structure and Physical Properties of Polyethylenes obtained from Dual Catalysis Process

J.F. Vega (✉), J. Otegui, M.T. Expósito, M. López[#], C. Martín[#] and J. Martínez-Salazar

Departamento de Física Macromolecular, Instituto de Estructura de la Materia, CSIC, Serrano 113 bis, 28006 Madrid (Spain)
[#]Centro de Tecnología Repsol-YPF, Carretera de Extremadura A5, Km 18, 28931 Móstoles, Madrid (Spain)
E-mail: imtv477@iem.cfmac.csic.es; Fax: +34 915 615 413

Received: 19 September 2007 / Revised version: 8 November 2007 / Accepted: 22 November 2007

Summary

Polyethylenes with bimodal molecular weight distribution were synthesized by using dual catalyst systems. It is found that the molecular weight and its distribution is highly influenced by the molar ratio between the two catalytic centres, and that a synergistic effect exists, being the molecular weight of the products higher than that corresponding to the materials obtained from the isolated catalysts. What it is interesting is that the molecular weight distribution shape, the microstructure and the final polymer properties could be regulated by the selection of this ratio. Results from this study show that materials with a broad range of microstructures, crystallinities and mechanical properties are obtained. The correlations found show that although a double population of macromolecular species exists, both are able to co-crystallize to form a unique crystalline structure from dilute solution. Rheological testing point towards a pronounced shear thinning behaviour, very high relaxation times, and thermorheological complexity, suggesting the incorporation of long chain branching during the polymerisation process. In addition, simple additive models applied to the linear viscoelastic properties of the polymers, by using the rheological response of the pure components, are unable to explain the experimental results obtained, suggesting a tandem effect rather than a dual action between the two active centres.

Keywords

dual catalysis, bimodal polyethylene, microstructure, mechanical properties, rheological behaviour

1. Introduction

Physical and chemical properties of polyethylene (PE) have been deeply investigated along the last decades. A major interest has been recently paid to PE with suitable properties for extreme environmental conditions and specific applications, in combination with high-quality processing. To approach these objectives, a monitoring of the molecular architecture should be considered, establishing useful relationships among specific polymerisation features, macromolecular attributes and physical properties. The main molecular feature to improve processing is to control the molecular weight distribution (MWD), being the highlights for the best quality bimodal or multimodal MWD [1,2]. Even the presence of very small long molecules in narrow MWD improves processability [3-5]. However, the requirement for enhanced mechanical properties in the solid state is the presence of short chain branches (SCB) along the longest chains of the distribution. The presence of side branches prevents molecules to come into the crystals, and then they are rejected to the amorphous and intercrystalline regions [2]. Conventional Ziegler-Natta catalysts do not incorporate SCB in the high molecular weight tail of the distribution, but rather in the shorter chains. For this reason, it is a usual practice to mix both linear-short and branched-long molecules in a physical blend [6]. Mixing of two catalysts can also be used to control polymer microstructure. This means that the polymerisation proceeds with the two catalytic centres in the same reactor, to allow a close interaction between both linear and branched species. In this context, tandem or dual catalysis is undergoing to a growing importance [7-10]. The current interest in this type of process is possible due to the recent progress in single-site catalysis (SSC), which has provided new PE grades, mainly regarding to the incorporation of SCB and the controlled MWD. A number of studies have been performed in the field of ethylene polymerisation and the study of the properties of polymers obtained by mixing two catalyst, either SSC, conventional, or both [1,11-21]. The objective of this work is to investigate the polymer structure and the properties of PE samples obtained from a dual catalysis process. The materials obtained from two different dual catalyst systems, formed by two different Brookhart iron catalyst (FeI and FeII) that incorporates only ethylene to form homopolymer, and one single-site metallocene catalyst based on zirconium able to incorporate ethylene and 1-hexene as comonomer (Zr), have been investigated. The influence of the dual system on polymer microstructure and physical properties has been studied. The polymers were analysed by GPC, ^{13}C-NMR, DSC, CRYSTAF, and mechanical and rheological testing.

2. Experimental

Catalysts and polymerisation conditions

The general formulations of the catalysts used are observed in Scheme 1. The catalysts were supported on SiO_2/MAO. The polymerisations were carried out in a Buchi

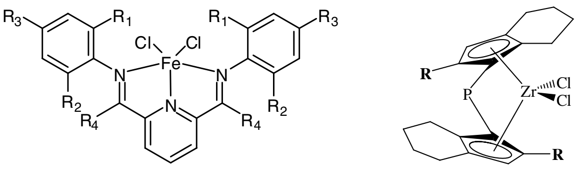

1a 1b

R1, R2, R3, R4, R5 y R6 = H, Me, Pr, ^{t}Bu, Bu, Cl
R = H, Me, Et, ^{i}Pr, Pr, ^{t}Bu
P = CH_2-CH_2-CH_2; CH_2-CH_2, CPh_2, CMe_2, $SiMe_2$, $SiMe_2CH_2$, $SiMe_2OSiMe_2$

Scheme 1. Chemical structures of the catalysts used in the polymerisations autoclave reactor. Isobutene solvent (1 dm^3) and the required amount of MAO co-catalyst were introduced into the reactor under inert nitrogen atmosphere. The total pressure was adjusted to 40 bars. Reaction was carried out at a temperature of 90ºC and kept constant throughout the polymerisation. The comonomer 1-hexene feed was 0.25 mol.

Polymer Characterization

All the samples were analysed by ^{13}C-NMR on a Bruker DRX 500 spectrometer. Molecular weights M_w and M_n and molecular weight distributions were determined by size exclusion chromatography (SEC) in a 150CV Waters GPC coupled with refractive index RI and viscosity detectors. The molecular characteristics of the polymers are listed in Table 1. Chemical composition distributions of the polymers were determined with a CRYSTAF/TREF instrument model 200+ (PolymerChAR, Spain). Please refer to previous work for experimental details [22].

Table 1. Molecular properties of polyethylenes obtained from experiences 1 and 2

Material_Fe/Zr ratio	1-hexene [mol-%]	M_w [kg mol^{-1}]	M_w [kg mol^{-1}]^a	M_w/M_n [-]	ρ [g cm^{-3}]^b
E1_1/0	0 (0)	99.1 [0]	-	39.5	0.9695
E1_2/1	0.17 (0.24)	185.6 [0.23]	450.0	105	0.9363
E1_1/1	0.37 (0.54)	374.4 [0.60]	>1000	100	0.9360
E1_1/2	0.67 (0.98)	280.9 [0.74]	>1000	90.0	0.9366
E1_0/1	0.68 (1)	335.0 [1]	>1000	3.5	0.9215
E2_1/0	0 (0)	31.0	-	5.3	0.9737
E2_2/1	0.25 (0.32)	n.d.	300.0	n.d.	0.9612
E2_1/1	0.33 (0.43)	n.d.	600.0	n.d.	0.9449
E2_1/2	0.54 (0.70)	n.d.	>1000	n.d.	0.9292
E2_0/1	0.77 (1)	n.d.	>1000	n.d.	0.9191

The values in ( ) are the calculated mole fraction of copolymer in the dual material from 1-hexene content. The values in [ ] are the calculated fraction of copolymer in the dual material from GPC traces.

n.d. means not determined.

[a] Rheological estimation assuming linear architecture

[b] Obtained from a gradient column

Thermal, mechanical and rheological properties

Differential scanning calorimetry (DSC) was performed on a Perkin-Elmer 7 series thermal analyser, and indium was used as a calibration standard. The nascent powder of the polymer was heated to 160°C (10°C/min), held at 160°C for 1 min, cooled to 25°C (10°C/min), and held at 25°C for 1 min. Finally; the polymer was heated to 160°C (10°C/min). The reported melting point is the peak value from the last heating. Crystallinity values were calculated using a value of 288.4 J/g was used as the reference melting enthalpy for 100% crystalline polyethylene [23]. The materials were stabilized using 0.1%-weight of 2,6-di-tert-butyl-4-methylphenol by mixing the copolymer and the antioxidant during compression moulding. The samples were sandwiched between metallic sheets, heated at 160ºC, held for 5 min under a nominal pressure of 150 kg/cm^2, and then quenched to room temperature. For mechanical and rheological testing suitable samples were punched out of the compression-moulded plates. Flexural dynamic stress-strain behaviour o in the solid state was obtained by dynamic mechanical spectroscopy analysis in a Perkin-Elmer 7 series analyser with the 3-point bending geometry at 25ºC.Rectangular shaped samples of about 15 mm × 5 mm × 1 mm were cut from the compression-moulded sheets. Complex flexural modulus, $|E^*_f|$, and loss angle, δ, at a frequency of 1 Hz were obtained in the linear viscoelastic range (strain< 1%). Small-amplitude oscillatory viscoelastic measurements in the melt were carried out in a Bohlin CVO stress-controlled rheometer using the parallel disk (15 diameter) geometry, in the angular frequency range between 6.28×10^{-4} and 6.28×10^{2} rad·s^{-1}, well inside the linear viscoelastic region, c.a. shear strain lower than 10 %. The following viscoelastic functions were measured as a function of the angular frequency, ω, at different temperatures: storage modulus, G'; loss modulus, G'', and phase angle, δ. The temperature range of measurements was from 130 to 190ºC. The time-temperature superposition principle has been applied to a reference temperature of 190ºC [24].

3. Results and discussion

Molecular weight and molecular weight distribution

The polymers produced using the different combinations of catalysts are characterised by a very broad and bimodal MWD. One can see in Figure 1 that the MWD obtained for the polymers generated in experience 1 (FeI/Zr), has two well-defined maxima centred at the characteristic values of the pure homo- and copolymer samples. Moreover, the polydispersity indices are very high, of the order of 100. It is interesting to note that the low molecular weight side of the distributions nearly remains around the maximum value of the pure homopolymer, independently of the Fe/Zr ratio. On the contrary, the maximum centred at the high molecular weight side shifts to considerable higher values as lower is the Fe/Zr ratio. It is remarkable the fact that the average molecular weight of the polymers synthesized with the dual catalyst system is of the same order of magnitude or higher, with one exception, than the corresponding to any of the individual catalysts (see Table 1). This could be an indication of an incorporation of material coming from the Fe sites in the growing chains of the Zr single-site centre. A similar situation has been recently reported for materials obtained from dual catalysis of two SSC systems [18]. This is a highly desirable feature of the combined system as high molecular weight of this component is necessary to improved mechanical properties of the materials.

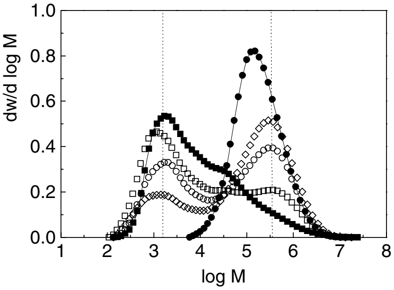

Figure 1. GPC traces of samples obtained in experience 1 (FeI/Zr). (■; E1_1/0); (□; E1_2/1); (O; E1_1/1); (◇; E1_1/2); (●; E1_0/1).

Chemical composition, thermal and mechanical properties

^{13}C NMR results for the polymers obtained are consistent with a branched molecular architecture (Table 1). The amount of branching due to the 1-hexene comonomer increases with decreasing the Fe/Zr ratio in the polymerisation. This suggests that the Fe catalyst only incorporates ethylene, in agreement with our computational studies [25], and that the copolymerisation is only possible when the Zr catalyst is present in polymerisation medium.

CRYSTAF profiles obtained for samples of experiences 1 (FeI/Zr) and 2 (FeII/Zr) reproduce the characteristic shape of homogeneous chemical compositions. In Figure 2a only those profiles obtained for samples from experience 2 are presented. The materials from experience 1 a show a nearly identical behaviour (see Figure 2b). This result noticeably differs from those obtained by GPC, in which a double population of molecular species is clearly seen (Figure 1). As the Fe catalytic centres are only able to incorporate ethylene, and Zr sites easily incorporates comonomer, a double population of crystals centred at 85°C for the linear molecules and at 79°C for the branched ones would be expected. The homogeneous CRYSTAF profiles of experiences 1 and 2 indicate a co-crystallisation phenomenon from dilute solution between linear and branched species. The weight average crystallization temperature, T_w, linearly decreases with the average content of 1-hexene in the materials measured by ^{13}C-NMR, in a similar way than in homogeneous SSC ethylene/1-hexene copolymers [26-28], as it can be observed in Figure 3.

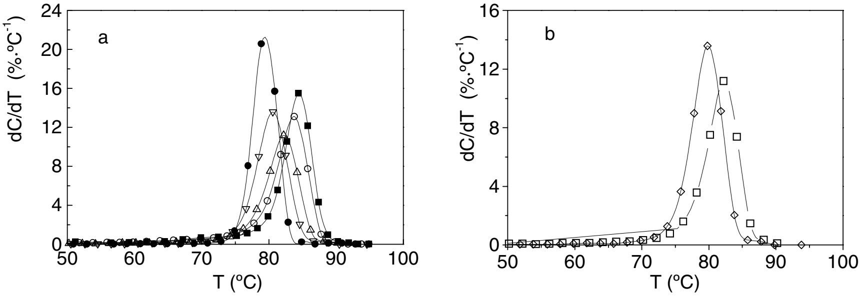

Figure 2. **(a)** CRYSTAF profiles of samples obtained in experience 2 (FeII/Zr): (■, E2_1/0); (O, E2_2/1); (△, E2_1/1); (▽,E2_1/2); (●,E2_0/1); **(b)** CRYSTAF profiles of dual samples from the two experiences with equimolar Fe/Zr ratio: (□, E1_1/1); (◇, E2_1/1).

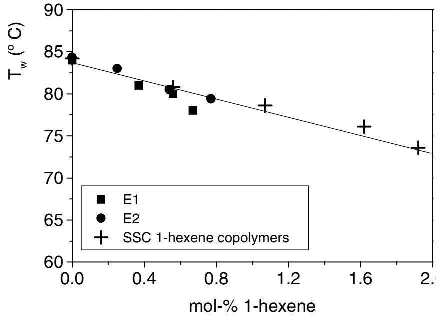

Figure 3. Correlation between the weight average crystallisation temperature and comonomer content from ^{13}C NMR measurements. The results are compared with those obtained for model SSC copolymers in our laboratory [28].

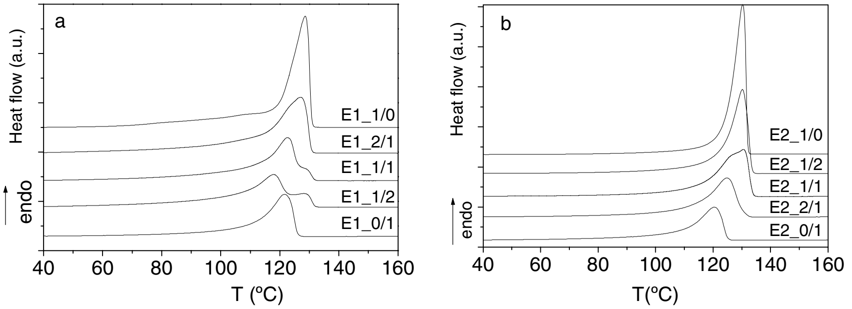

Figure 4. DSC traces of materials obtained in **(a)** experience 1 and **(b)** experience 2.

DSC analysis reveals that the products obtained from the different catalysts combinations exhibit different thermal properties. In Figures 4a and 4b the DSC traces of pure components and dual samples from the different experiences are presented. DSC traces support the result obtained from CRYSTAF analysis only in the case of the materials obtained in experience 2, as it can be observed in Figure 4b. The samples obtained in experience 1 (Figure 4a) show two melting peaks, corresponding to a double population of crystals. Materials with equimolar Fe/Zr ratio from the two experiences can be compared in Figures 4a and 4b. A very different M_w of both low and high M_w fractions could originate the double population of crystals in the material of experience 1 (see the results obtained for E1_1/2 and E1_1/1 samples). It is worthwhile to mention that this phenomenon is more pronounced as MWD broadens (Table 1 and Figure 4a). The molecular species of the materials obtained from experience 2 co-crystallize even from the melt state, likely due to lower difference between molecular sizes of the involved species. The different catalyst combinations have lead to products with different molecular architecture, and then physical properties should be also influenced. A nice correlation has been found between the crystal content of the samples and density, as it is observed in Figure 5a. The results obtained compares well with data obtained in our laboratory for SSC metallocene ethylene/1-hexene copolymers. In the same way, comparable trends have been found for the flexural modulus, which linearly increases as crystal content and density do

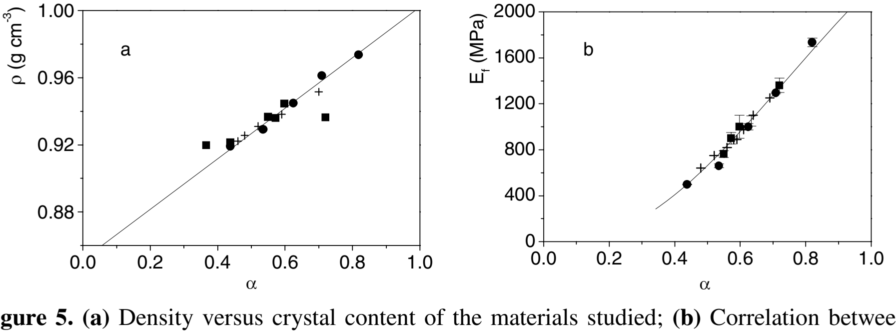

Figure 5. **(a)** Density versus crystal content of the materials studied; **(b)** Correlation between flexural modulus obtained in dynamic mode and crystal content. Symbols are the same than in previous figures. The results are compared with those obtained for model SSC copolymers.

(see Figure 5b). This trend is again nearly identical to that observed in single-site catalysed ethylene/1-hexene copolymers with homogeneous microstructure. All these results seem to indicate that although a bimodal distribution of molecular lengths and a double population of linear and branched species exists, the ultimate structural parameter that controls physical properties is crystallinity and the ability of both molecular species to co-crystallize. These observations are in agreement with previous results in our group, which indicate that the mixing of both linear and branched species takes place whenever the branching content is lower than 4 %-mol [29].

Rheological properties

The homopolymer and the copolymer obtained from pure catalysts show a very different viscoelastic fingerprint in linear rheology. The results obtained at 190ºC can be observed in Figure 6 for both products of experience 2. Similar results are obtained for the pure samples in experiences 1, with only small variations due to some differences attributed to slightly different M_w and/or MWD. The strong difference between both pure components can be explained by the very different molecular architecture. No cross-point between G' and G" is observed for the samples, but this is due to different reasons. The homopolymer shows the typical behaviour of a low M_w and a broad MWD sample, with an important fraction of unentangled chains (bellow the critical molecular weight for entanglements, M_c~3000 g mol^{-1}), then this polymer shows a viscous behaviour in the whole range of frequencies experimentally available at this temperature. On the contrary, the copolymer shows a characteristic elastic behaviour far beyond the expected for a single-site catalysed polymer sample with a narrow MWD. G' is higher G" in the whole range of frequencies explored, and the cross-point between them is shifted to very low frequencies, lower than $\omega_x = 10^{-2}$ rad s^{-1}. These very low values of the cross-point frequency are typical of ultra-high molecular weight polymers ($M_w > 10^6$ g·mol^{-1}) or long chain branched products, for which reptation is highly suppressed. The difference is also clear when complex viscosity values are compared. This viscoelastic feature shows a strong dependence on angular frequency, as it is typical of polymer samples with broad MWD and/or long chain branching. Pure copolymers do not show the expected levelling off of the complex viscosity at very low frequencies, and the viscosity values are four orders of magnitude higher than in the homopolymer.

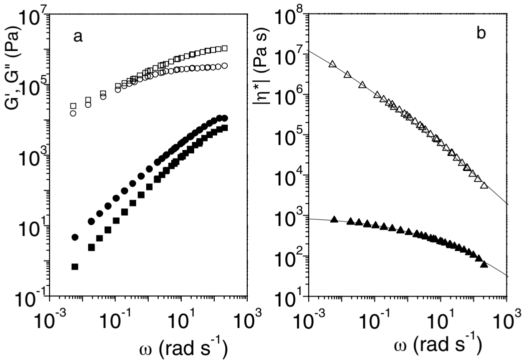

Figure 6. **(a)** Storage and loss moduli, and **(b)** complex viscosity of pure polymers (open symbols: E2_0/1; close symbols: E2_1/0) of experience 2. The lines are drawn to guide the eye.

As it is observed in Figure 7a characteristic dilution of the linear viscoelastic response of the materials is observed as the Fe/Zr ratio increases. The dilution effect is seen as lower absolute values of the shear complex modulus (G' and G"), and also with the development of a more viscous character of the products (G" is higher than G' in a broader frequency range). Moreover, the cross-point between G' and G" appears, for a given Fe/Zr ratio of 1, and the characteristic frequency, ω_x, shifts to higher values as Fe/Zr increases. As the reciprocal cross-point frequency can be taken as an average relaxation time, $\tau_x=1/\omega_x$, a characteristic decrease of the relaxation time of the samples proceeds as Fe/Zr ratio increases. For linear polyethylenes with narrow MWD, the decrease of τ_x is directly related with a decreased M_w. The calculated M_w (obtained from the ω_x *versus* M_w relationship of linear polyethylene) varies between 300 and higher than 1000 kg·mol^{-1} as Fe/Zr decreases for the materials in Figure 7b [30]. These values are actually higher than those obtained from GPC, and can be read as a signature of the presence of LCB in the samples studied. A clear signature of the presence of LCB in the samples is obtained applying the time-temperature superposition principle (TTSP). The dual products are thermorheologically complex, as it is observed in Figure 8 (only one case is shown).

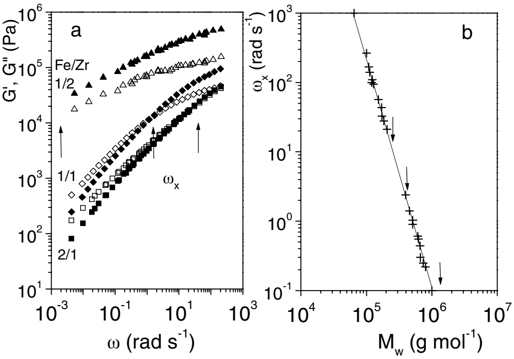

Figure 7. **(a)** Effect of Fe/Zr ratio on storage and loss moduli of the dual samples obtained from experiences 1 and 2: (△: E1_1/2; ◇: E2_1/1; □: E2_2/1). **(b)** Estimation of M_w of some of the samples from results of model SSC polyolefins [30]. The arrows indicate the location of the cross-point frequency.

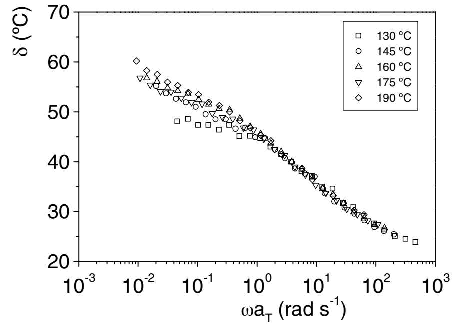

Figure 8. Phase angle versus reduced angular frequency at 190ºC for one of the samples obtained in experience 1 (E1_1/2). The different symbols correspond to temperatures between 130 and 190ºC.

TTSP does not apply, and the viscoelastic properties are more sensitive to temperature in the low frequency zone. This means that the temperature dependence, and then the flow activation energy E_a, is different depending on the frequency regime, in agreement with previous observations made for LCB polyolefins by Wood-Adams and Costeux [31]. These authors found different activation energy spectra for different LCB polymeric samples depending on molecular architecture (short and long chain branching content). Then, the complex thermorheological behaviour will arise from multiple mechanisms with different temperature dependencies. For the materials studied here the complexity likely comes out as a result of different populations of linear and (long) branched species.

Modelling of the linear viscoelastic response: molecular architecture

As the macromolecular species growth at the same time in the reaction medium one would expect intimate interaction between both linear and branched species in the final products. This segmental interaction will affect the rheology, being the linear viscoelastic response consistent with existing theories on molecular dynamics for homogeneous blends of polymeric materials. We can adequately describe the rheological behaviour of a blend on basis of the double reptation concept, taking into account the linear viscoelastic response of the individual species in the mixed blend. The assumed blending law for the double reptation to the relaxation modulus, *G(t)*, for homogeneous mixtures of *i* components with individual relaxation modulus $G_i(t)$ is given by the expression [32]:

$$G(t) = \left[\sum_{i} w_i G_i^{1/c}(t) \right]^{c} \qquad \textbf{(1)}$$

The parameter C equals to 2 in the original Tsenoglou rule for double reptation [33,34], but it has been found to vary between 1.25 and 3.84, depending on the polymeric systems mixed and the mathematical approach adopted [6,32,38-37]. The individual relaxation modulus, $G_i(t)$, can be obtained by Fourier transform of the experimental data of *G′* and *G″* of the pure polymers. From the calculated *G(t)* for the dual samples by using equation 1, the theoretical values of *G′* and *G″* can be also easily obtained upon the application of the same procedure. The results are shown in Figure 9a. We have selected the materials obtained from experience 2, as these samples show the broader range of variation in the linear viscoelastic features, from the very elastic limit (pure copolymer) to the very viscous one (pure homopolymer). We have applied equation 1 using the results of the pure components and their calculated weight fractions from 1-hexene content. The model is not able to explain the viscoelastic behaviour of the samples studied, even considering an arbitrary compositional fraction of the linear and branched species. This suggests that the mixed species in the dual materials exhibit a different molecular architecture than the pure components. The different molecular architecture is probably due to a tandem action of the Zr active centres, not only able to incorporate ethylene and 1-hexene, but also any other vinyl terminated species present in the reaction medium, generated by the Fe active centres. The model has been also applied to the experimental complex viscosity at a fixed angular frequency of 0.01 rad·s^{-1} for all the dual samples under study in Figure 10b. The model does not explain the viscosity variation of the samples with the copolymer fractional content, but an interesting general trend is observed as

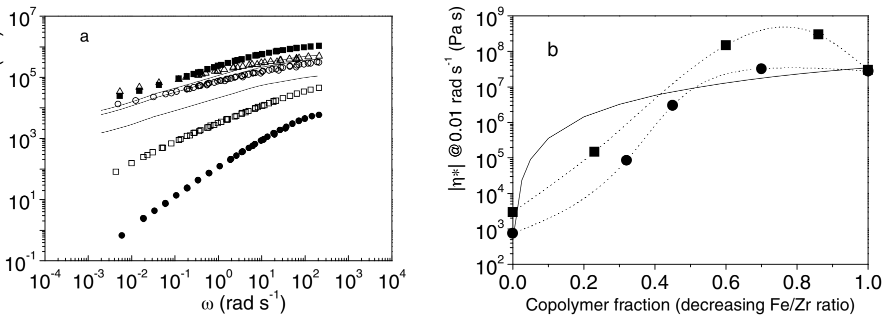

Figure 9. **(a)** Application of double reptation model for homogeneous blends to storage moduli of the products obtained in experience 2: Close symbols: pure materials (■) E2_0/1 and (●) E2_1/0; open symbols: dual polymers (□, E2_2/1); (O, E2_1/1); (△, E2_1/2); **(b)** Variation of complex viscosity at a fixed angular frequency for the materials obtained from the different experiences as a function of the copolymer fraction. (■) Experience 1 and (●) experience 2. The solid line represents the expected variation of the viscosity with the copolymer fraction by assuming the mixing rule given by equation 1.

Fe/Zr ratio increases. In both cases a clear positive deviation is seen for the samples with the highest content in copolymer fraction. This is a signature of the tandem effect occurring between both active centres during the polymerisation. This is likely due to the incorporation of vinyl-terminated chains coming from the Fe active centres to the chains growing in the Zr active ones. This would give rise to complex long chain branches structures, characterized by long relaxation times and higher viscosities than the pure copolymer. The effect is much more pronounced in the case of the samples obtained in experience 1. We have to point out here that the homopolymer species are longer in this case than in experience 2 (higher values of M_w and viscosity, as it is observed in Table 1 and in Figure 9b).

4. Conclusions

The different catalysts systems studied generate broad and bimodal molecular weight distributions. Moreover, an increase of the molecular weight of the dual polymers is observed with respect to that obtained in the polymers using the isolated catalysts. This is probably due to synergistic interaction of both systems, which gives rise to the incorporation of a fraction of the linear polymer from Fe centres to the growing chain from Zr centres. ^{13}C-NMR results showed the increased presence of 1-hexene comonomer in the materials as the Fe/Zr ratio in the polymerisation decreases, then it seems that only single-site Zr centres incorporates comonomer. The comonomer distribution obtained from CRYSTAF and DSC analysis did not allow corroborating the double population of species obtained from GPC measurements. There is no a clear correspondence between thermal properties obtained from CRYSTAF and DSC, which can be explained as due to a co-crystallisation phenomenon from dilute solution of both molecular species. The mechanical properties of the materials studied only depend on structural parameters as crystallinity and consequently density. A linear dependence of the flexural modulus with both parameters has been found. The rheological study showed that the materials show complex thermorheological behaviour. The application of molecular models from the experimental data of pure components, assuming segmental interaction between molecular species, is not able to describe the rheological response. This results suggest that the molecular architecture of the components in the materials (mainly the copolymer species obtained from single-site Zr centres) is different from that corresponding to the pure components obtained from the isolated catalysts, due to a tandem action between both active centres.

Acknowledgements. Thanks are due to the CICYT (MAT2006-0400 project) and CAM (S-0505-PPQ/0328-02) for financial support. J.F. Vega acknowledges the MEC for a Ramón y Cajal Tenure (2006). J. Otegui thanks the CSIC (Post-graduate I3P Program) for the tenure of a fellowship. M.T. Expósito thanks the MEC for a Ph.D. fellowship (2003).

References

1. Muñoz-Escalona A, Lafuente P,Vega JF, Santamaría A (1999) Polym Eng Sci 39:2292
2. DesLauriers PJ, McDaniel MP, Rohlfing DC, Krishnaswamy RK, Secora SJ, Benham EA, Maeger PL, Wolfe AR, Sukhadia AM, Beaulieu BB (2005) Polym Eng Sci 45:1203
3. Aguilar M, Expósito MT, Vega JF, Muñoz-Escalona A, Martínez-Salazar J (2004) Macromolecules 37:681
4. Aguilar M, Martín S, Vega JF, Muñoz-Escalona A, Martínez-Salazar J (2005) J Polym Sci Polym Phys 43:963
5. Barrera MA, Vega JF, Aguilar M, Martínez-Salazar J (2006) J Mat Process Technol 174: 171
6. Peón J, Domínguez C, Vega JF, Aroca M, Martínez-Salazar J (2003) J Mat Sci 38:4757
7. Commereuc D, Hugues F, Le Quan N, Taouli A (1988) US Patent No 4721762
8. Pettijohn TM, Reagen WK, Martin SJ (1995) US Patent No 5393719
9. Michiels W, Muñoz-Escalona A (1996) European Patent No 0719797
10. ReagenWK, Pettijohn TM, Freeman JW, Benham EA (1998) US Patent No 5786431
11. Ahlers A, Kaminsky W (1988) Makromol Chem Rapid Commun 9:457
12. Heiland K, Kaminsky W (1992) Makromol Chem 193:601
13. Han TK, Choi HK, Jeung DW, Ko YS, Woo SI (1995) Macromol Chem Phys 196:2637
14. D'Agnillo L, Soares JBP, Penlidis A (1998) J Polym Sci Polym Chem36:831
15. Kim JD, Soares JBP, Rempel GL (1999) J Polym Sci Polym Chem 37:331
16. Liu J, Rytter E (2001) Macromol Rapid Commun 22:952
17. Quijada R, Rojas R, Bazán G, Komon ZJA, Mauler RS, Galland GB (2001) Macromolecules 34: 241
18. Dekmezian AH, Soares JBP, Jiang P, Garcia-Franco CA, Weng W, Fruitwala H, Sun T, Sarzotti DM (2002) Macromolecules 35:9586
19. Bruaseth I, Rytter E (2003) Macromolecules 36: 3026
20. de Wet-Roos D, Dixon JT (2004) Macromolecules 37: 9314
21. Lu ZX, Zhang Z, Li Y, Wu C, Hu Y (2006) J Appl Polym Sci 99: 2898
22. Expósito MT, Vega JF, Martínez-Salazar J (2007) in press J Appl Polym Sci
23. Quinn FA Jr, Mandelkern L (1958) J Am Chem Soc 80:3178
24. Mavridis H, Shroff R (1992) Polym Eng Sci 132:1778
25. Ramos J, Cruz V, Muñoz-Escalona A, Martínez-Salazar J (2002) Polymer 43: 363
26. Sarzotti DM, Soares JBP, Penlidis A (2002) J Polym Sci Polym Phys40:2595
27. Sarzotti DM, Soares JBP, Simon LC, Britto LJD (2004) Polymer45:4787
28. Expósito MT (2006) Ph.D. Thesis, Universidad Complutense de Madrid
29. Martínez-Salazar J, Sánchez Cuesta M, Plans J (1991) Polymer 32:984
30. Vega JF, Aguilar M, Martínez-Salazar J (2003) J Rheol 47:1505
31. Wood-Adams P, Costeux S (2001) Macromolecules 34:6281
32. Lee HS, Denn MM (2000) Polym Eng Sci 40:1132
33. des Cloizeaux J (1988) Europhys Lett 5:437

34. Tsenoglou C (1991) Macromolecules 24:1762
35. Groves DJ, McLeish TCB, Choham RK, Coates PD (1996) Rheol Acta 35:481
36. Maier D, Eckstein A, Friedrich C, Honerkamp J (1998) J Rheol 42:1153
37. Thimm W, Friedrich C, Marth M, Honerkamp J (1999) J Rheol 43:663